



# High Velocity Outflows in Intrinsic Narrow Absorption Line Quasars

## Summary

High velocity and massive outflowing winds may be present in most quasars but only detected in those cases where our line of sight intersects the outflowing absorbing stream. We present results from *Suzaku* and *XMM-Newton* observations of a sample of Intrinsic Narrow Absorption Line (NAL) quasars with high velocity outflows. In contrast to Broad Absorption Line (BAL) quasars we do not detect any significant excess intrinsic absorption in NAL quasars and the maximum outflow velocities of the UV absorbers of NAL quasars do not appear to be correlated with their X-ray weakness. Combining the results from X-ray observations of NAL and BAL quasars we present a unified picture to describe the outflow properties of both classes of objects. Our *Suzaku* and *XMM-Newton* observations of NAL quasars have allowed us to place tighter constraints on correlations between the X-ray weakness and UV properties of the wind to better understand the geometry and acceleration mechanism of quasar winds.

This work was supported by NASA through grants NNX07AF59G and NNX07AQ64G.

## Outflow Models

In the Elvis 2000 quasar outflow scenario, shown in Figure 1, NAL quasars are viewed at inclination angles larger than those of BAL quasars. This scenario also predicts NAL column densities that are comparable to those of BAL quasars (i.e., up to  $10^{23}$  cm $^{-2}$ ). In the Ganguly et al. (2001) scenario, shown in Figure 1, NALs are purported to arise in clumps of gas produced in the shearing zone between the outflowing gas and a highly-ionized, lower-density, unshielded medium. As a consequence, NALs are generally observed in quasars with systematically smaller inclination angles than BAL quasars, but can also be observed along side BAL quasars. Our line of sight towards NAL quasars in the Ganguly et al. scenario passes through less dense material with expected column densities in the range of  $10^{21-22}$  cm $^{-2}$ , 1-2 orders of magnitude less than that predicted in the Elvis scenario.

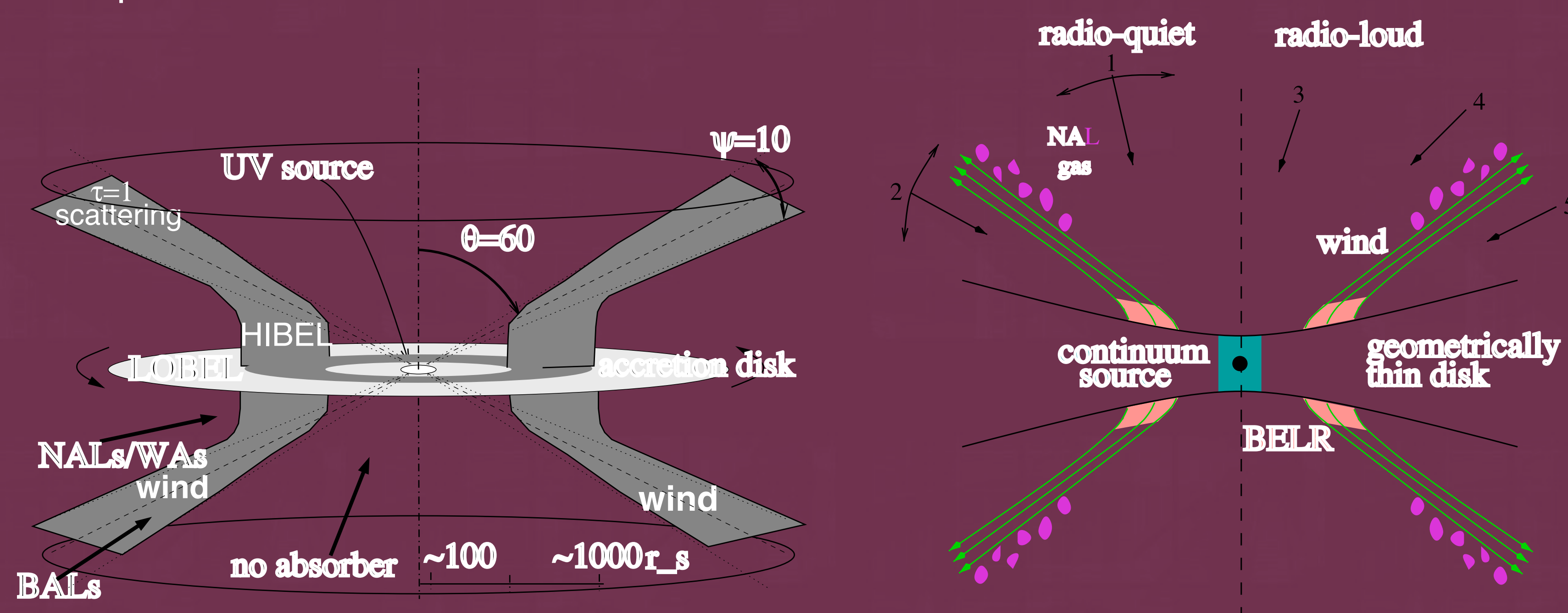


**Figure 1** – **left:** A paradigm for quasar atmospheres from Elvis (2000). **right:** Disk wind scenario for quasars from Ganguly et al. (2001).

## *Suzaku* and *XMM-Newton* Observations of Intrinsic NAL Quasars

For the purpose of our study we observed a sample of NAL quasars with *Suzaku* and *XMM-Newton*. A log of the observations that includes object name, observation dates, observatory, observed counts, effective exposure times, and observational identification numbers is presented in Table 1.

Object	Observation Date	Observatory	Observation ID	Effective	
				Exposure Time <sup>a</sup> (ks)	$N_{sc}$ <sup>b</sup>
Q0450-1310	2008 March 10	<i>Suzaku</i>	702062010	7.5	106 ± 10
Q0450-1310	2007 August 10	<i>XMM-Newton</i>	0503350301	5.88	242 ± 16
Q1009+2956	2007 October 31	<i>XMM-Newton</i>	0503350201	5.69	487 ± 22
Q1017+1055	2007 November 27	<i>Suzaku</i>	702064010	8.13	131 ± 12
Q1334-0033	2007 July 14	<i>Suzaku</i>	702067010	12.11	231 ± 15
Q1548+0917	2008 Feb 02	<i>Suzaku</i>	702068010	30.48	612 ± 25
Q1946+7658	2007 July 13	<i>Suzaku</i>	702060010	11.66	431 ± 21
Q1946+7658	2007 July 11	<i>XMM-Newton</i>	0503350101	2.96	200 ± 14

**Notes on Table 1** – (a) Effective exposure time is the time remaining after the application of good time-interval (GTI) tables to remove portions of the observation that were severely contaminated by background. (b) Background-subtracted source counts including events with energies within the 0.2-10 keV band. The source counts and effective exposure times for the *Suzaku* and *XMM-Newton* observations refer to those obtained with the combined XIS units and EPIC PN instrument, respectively.

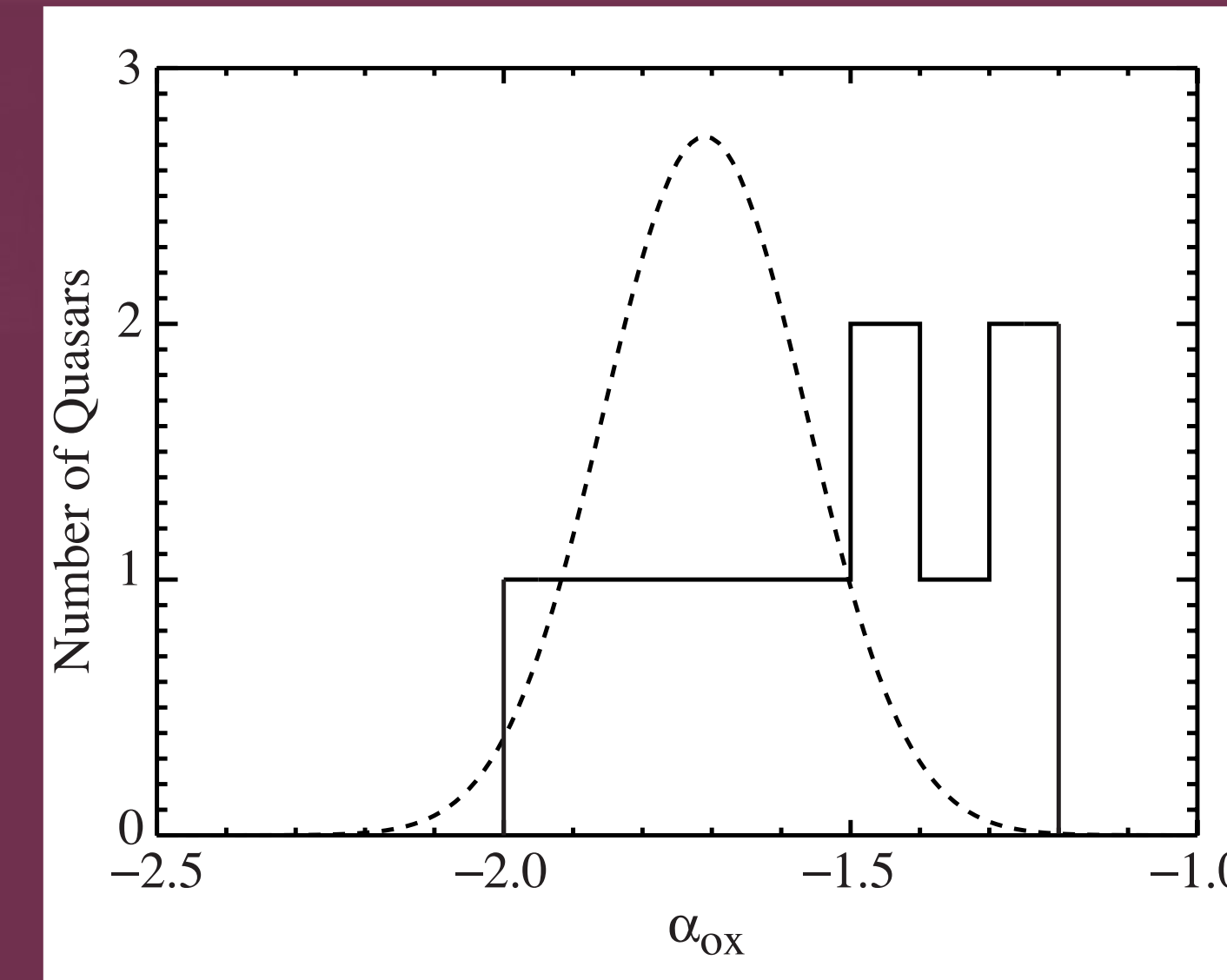


**Figure 2** – The distribution of values of  $\alpha_{\text{ox}}$  of NAL quasars without correction for intrinsic UV absorption. Six quasars in this sample are from this study and four are from the Misawa et al. (2008) study. The dashed line shows the distribution of non-absorbed radio-quiet quasars with UV luminosities similar to those of our sample (Steffen et al. 2006).

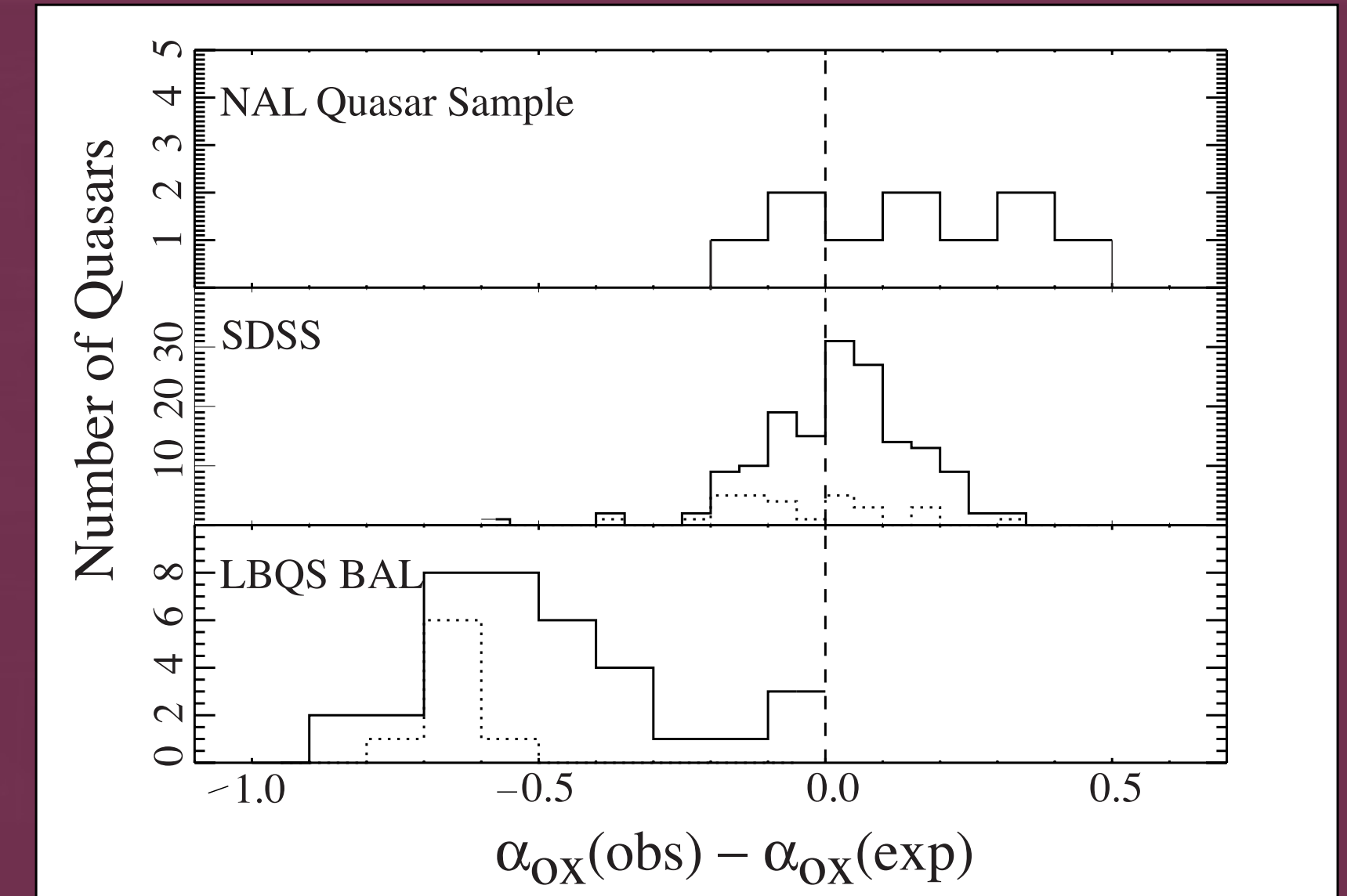


**Figure 3** – Distributions of  $\Delta\alpha_{\text{ox}}$ , the difference between the observed value of  $\alpha_{\text{ox}}$  and the value predicted for that monochromatic UV luminosity by the correlation of Steffen et al. (2006). Histograms drawn as dotted lines indicate upper limits. *Top:* The distribution of  $\Delta\alpha_{\text{ox}}$  among NAL quasars. *Middle:* The distribution of  $\Delta\alpha_{\text{ox}}$  among SDSS quasars (Steffen et al. 2006). *Bottom:* The distribution of  $\Delta\alpha_{\text{ox}}$  among BAL quasars from the LBQS (Gallagher et al. 2006).

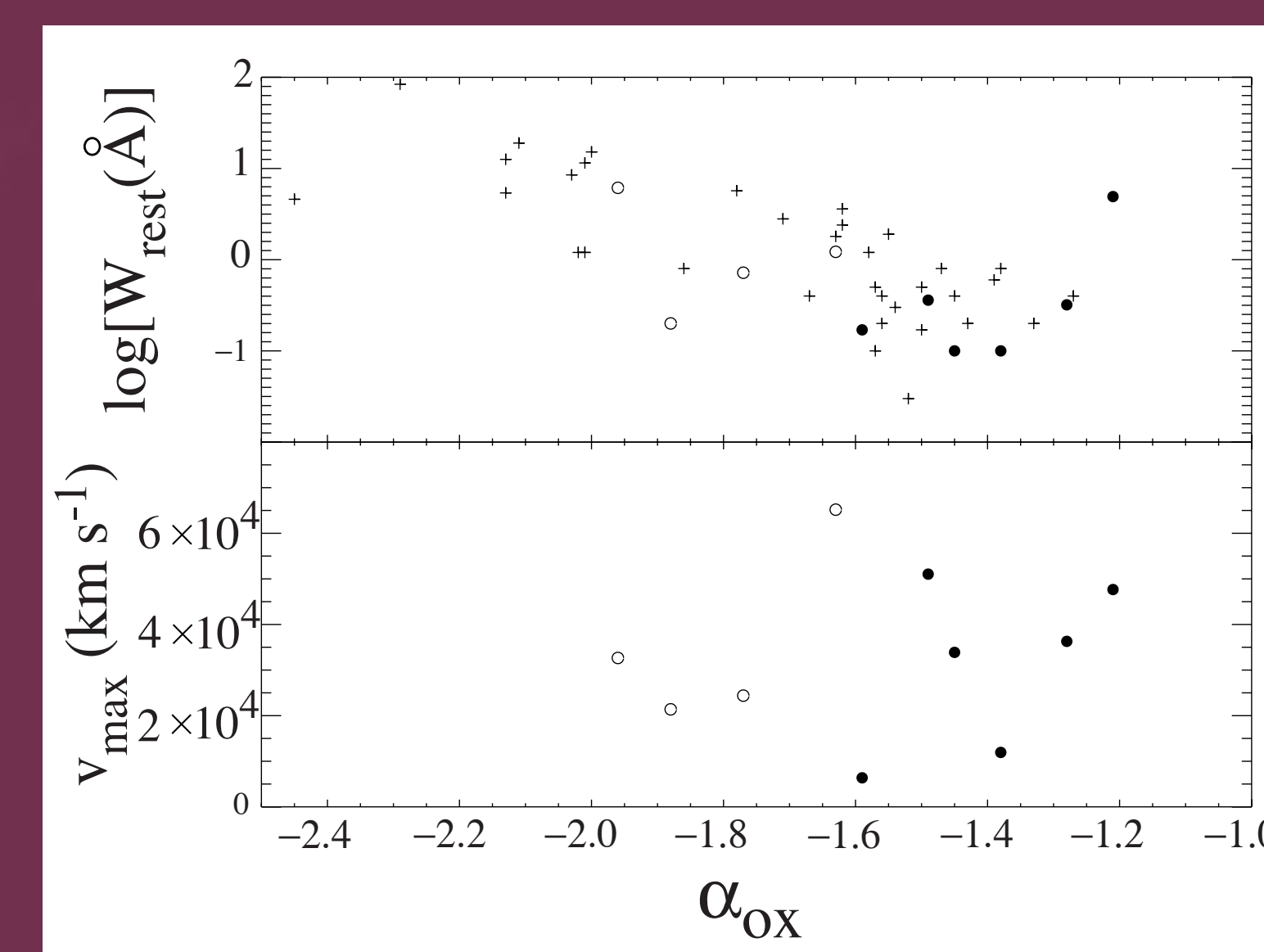


**Figure 4** – Properties of intrinsic C IV NALs of quasars in our sample (filled circles) and the Misawa et al. (2008) sample (open circles) plotted against  $\alpha_{\text{ox}}$ . *Top:* Variation of  $W_{\text{rest}}$  with  $\alpha_{\text{ox}}$ .  $W_{\text{rest}}$  is the sum of equivalent widths of all intrinsic NALs in the same quasar. The crosses represent the associated C IV NALs measured in low-redshift quasars by Brandt et al. (2000). *Bottom:* Variation of the maximum NAL velocity with  $\alpha_{\text{ox}}$ .

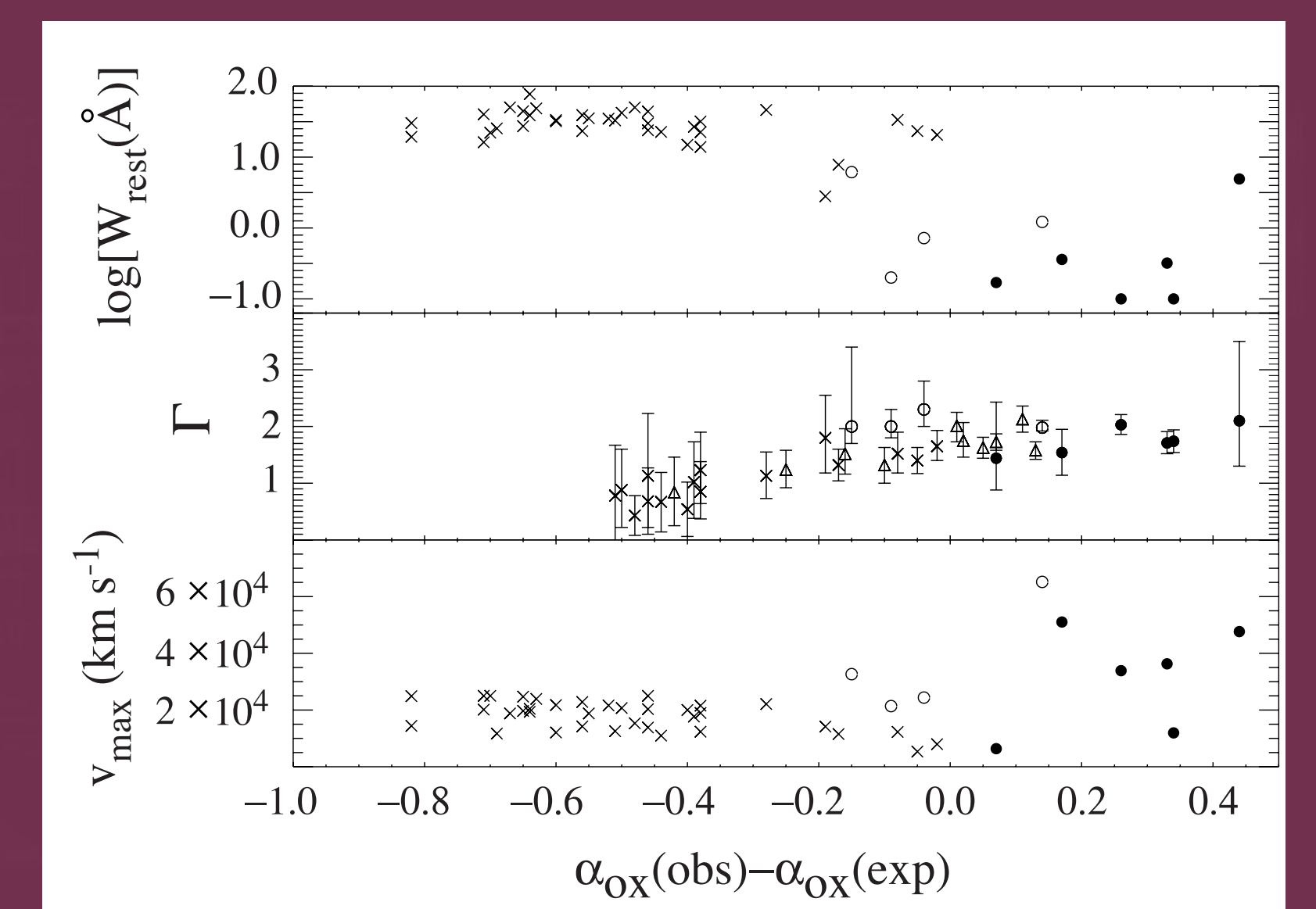


**Figure 5** – Comparison of the properties of quasars in our sample (filled circles) and the Misawa et al. sample (open circles) with the properties of BAL quasars from the sample of Gallagher et al. (2006). *Top:* Variation of  $W_{\text{rest}}$  with  $\Delta\alpha_{\text{ox}}$ . *Middle:* Variation of X-ray photon index with  $\Delta\alpha_{\text{ox}}$ . Open triangles in this panel represent the extremely red quasars from Hall et al. (2006). *Bottom:* Variation of the maximum NAL velocity with  $\Delta\alpha_{\text{ox}}$ .

## Results

- 1. The intrinsic column densities of the X-ray absorbers in our sample of NAL quasars are constrained to be less than a few  $\times 10^{22}$  cm $^{-2}$ . These values of  $N_{\text{H}}$  are consistent with the Ganguly et al. quasar outflow scenario in which NAL quasars are viewed at smaller inclination angles than BAL quasars.
- 2. The distributions of  $\alpha_{\text{ox}}$  and  $\Delta\alpha_{\text{ox}}$  of the NAL quasars of our sample differ from those of BAL quasars (Figures 2 and 3). The NAL quasars are not significantly absorbed in the X-ray band and the positive values of  $\Delta\alpha_{\text{ox}}$  suggest absorption in the UV band.
- 3. The positive values of  $\Delta\alpha_{\text{ox}}$  of the intrinsic NAL quasars can be explained in a geometric scenario where NAL quasars are viewed at low inclination angles (Figure 1 right panel). In this scenario, lines of sight towards a compact X-ray hot coronae of NAL quasars do not traverse the absorbing wind whereas lines of sight towards their UV emitting accretion disks do intercept the outflowing absorbers.
- 4. The maximum outflow velocities of the UV absorbers of NAL quasars are not correlated with their X-ray weakness in contrast to what has been reported for BAL quasars (i.e., Gallagher et al. 2006).
- 5. The total equivalent width,  $W_{\text{rest}}$ , summed over all the intrinsic C IV NALs in the same quasar when plotted versus  $\alpha_{\text{ox}}$  appears to follow the trend of  $W_{\text{rest}}$  vs.  $\alpha_{\text{ox}}$  found by Brandt et al. in nearby NAL quasars. The only outlier to this trend is quasar Q1017+1055 which contains both a NAL and mini-BAL absorber.